

## STRESS ANALYSIS OF CORROSION PITS PRESENT ON CURVED AND PLANE SURFACES CONSIDERING PLASTICITY

**Ricardo J. Bertin, João E. Abdalla Filho, Roberto D. Machado**

*Programa de Pós-Graduação em Engenharia Mecânica, Pontifícia Universidade Católica do Paraná - PUCPR, R. Imaculada Conceição, 1155, 80.215-901, Curitiba, Paraná, Brazil*  
*ricardo.bertin@pucpr.br, joao.abdalla@pucpr.br, roberto.machado@pucpr.br*  
<http://www.pucpr.br/ppgem>

**Keywords:** Pit corrosion defect, Pit defect stress analysis, Pipeline, Finite element analysis.

**Abstract.** Corrosion pits are insidious defects because they are difficult to detect due to their minute dimensions and because they act as stress intensifiers. In any steel structure, corrosion is always a major problem researched all around the world. The present study, investigates the stress distribution at a semi-elliptical corrosion pit on steel under static load using finite element analysis. A series of three-dimensional semi-elliptical pits are modeled by means of a systematic variation of the aspect ratio ( $a/2c$ ) where  $a$  is depth and  $c$  is radius, both on a curve surface of a pipeline and on a straight block, for various tensile loadings. It is being considered non linearity of the material. The research attempts to correlate results from curved surface to plane ones.

## 1 INTRODUCTION

Engineering main function, even before the term has been used for the first time, is the satisfaction of society needs. Such needs include housing, transportation, machinery, systems and tools, just to mention but a few. The list although finite is vast. To attain this very objective a lot of planning, careful analysis and design, and inspection, monitoring and maintenance must be made. Further, when detected, flaws and defects in structures must be evaluated. This work attempts to expand the knowledge about a specific type of defect known as corrosion pit from the stress distribution point-of-view. Corrosion pits are "very localized corrosion attacks in which little holes or pits are formed" (Callister, 2006). It is an insidious defect due to its minute dimensions that allows it to pass undetected. Because it is a stress intensifier corrosion pit may lead to fracture of the material (Turnbull, McCartney and Zhou, 2008), fatigue cracking (Pao, Gill and Feng, 2000) and rupture, even for defects smaller than a millimeter. It had been concluded (Cerit, Genel and Eksi, 2009) that the aspect ratio ( $a/2c$ ) of the pit, in other words, the relation between its depth ( $a$ ) and its opening ( $2c$ ) is "a main parameter affecting the value of SCF" where SCF stands for stress concentration factor. Working with corrosion pits on oil pipelines Bertin, Abdalla and Machado, (2009) derived a logarithmic relation relating maximum stress, ultimate tensile stress and aspect ratio.

## 2 OBJECTIVE

In this work maximum stress in corrosion pits on curved solids, like oil pipes, and on straight solids will be compared considering plasticity of material. An equation unifying both cases will be addressed.

## 3 METHODOLOGY

### 3.1 3D modeling

A straight solid is modeled as a solid steel block with dimensions 500 x 200 x 150 mm. A pit is centered on a 500 x 200 mm face as shown in Fig. 1.

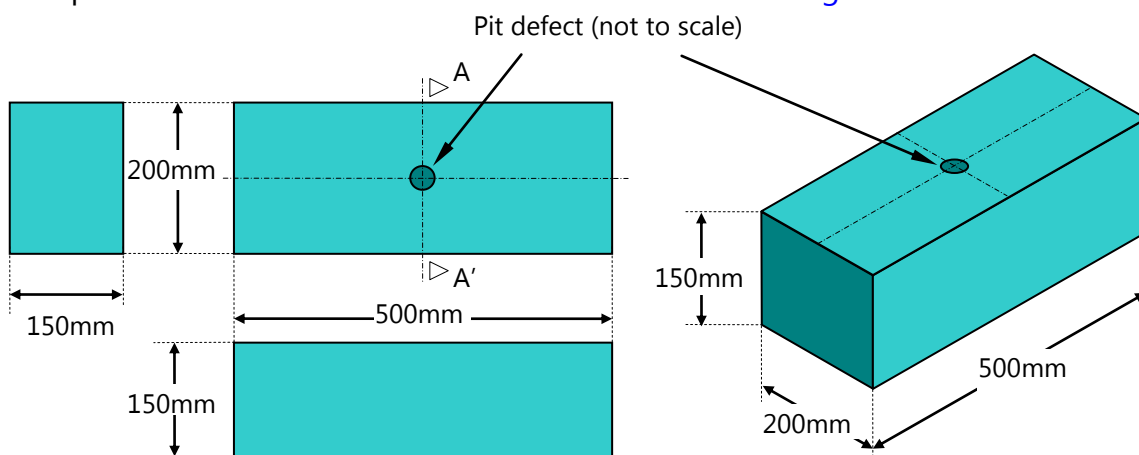


Fig. 1 – Dimensions and details of the solid block modeled, including pit position.

A curved solid is modeled as a stretch of 1000 mm of a pipe API L5 X60 with diameters of 300, 400 and 500 mm, and wall thickness of 15 mm. The pit is centered longitudinally on the external surface as shown in Fig. 2.

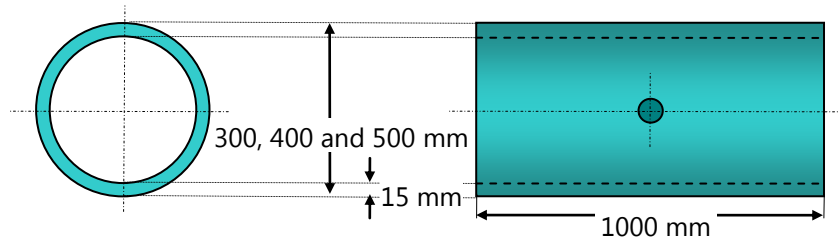


Figure 2 – Dimensions of the API L5 X60 steel pipe containing a pit.

On both cases it is taken advantage of two axis symmetry. Therefore only  $\frac{1}{4}$  of a semi-ellipsoid pit as shown in Fig. 3 is modeled.

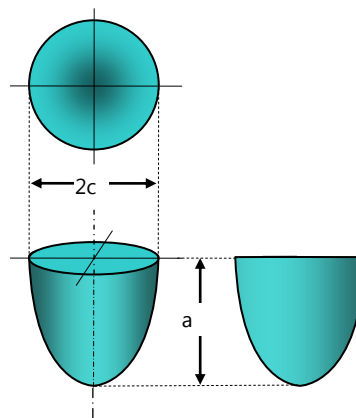


Figure 3 – Semi-elliptical surface modeling of the pit.

The following material properties are employed: Young's Modulus,  $E = 210,000$  MPa, Poisson's ratio,  $\nu = 0.3$ , yield stress,  $\sigma_{ys} = 483$  MPa, ultimate tensile strength,  $\sigma_u = 597$  MPa. A Von Mises plasticity model with stress – strain data depicted in Fig. 4 has been adopted.

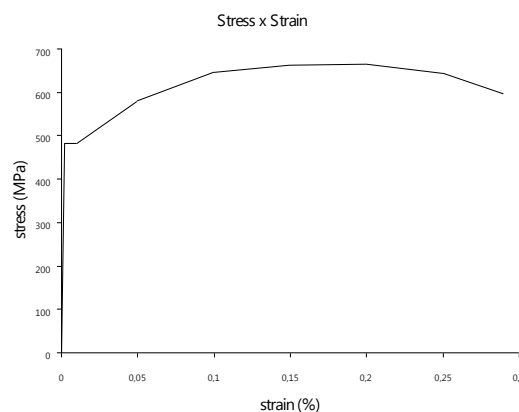


Figure 4 – API L5 X60 steel stress - strain curve.

### 3.2 ANSYS model

Finite element simulations using commercial program ANSYS<sup>®</sup> are performed. Meshing employs 3D 10-node tetrahedral structural solid elements. The 3-D model used in ANSYS<sup>®</sup> is constructed bottom up, in other words, defining points, lines, areas and volume using symmetry on both axes. On the solid block model depicted in Fig. 5 the longitudinal dimension, 250mm, is oriented along Z direction, with one corner, the lower right, located at the origin. Translation restraints are applied on areas, rather than on nodes or keypoints. Area on plane XY that includes the pit is Z restrained. Area XY where load is applied is X and Y restrained to prevent rigid body motion along these directions.

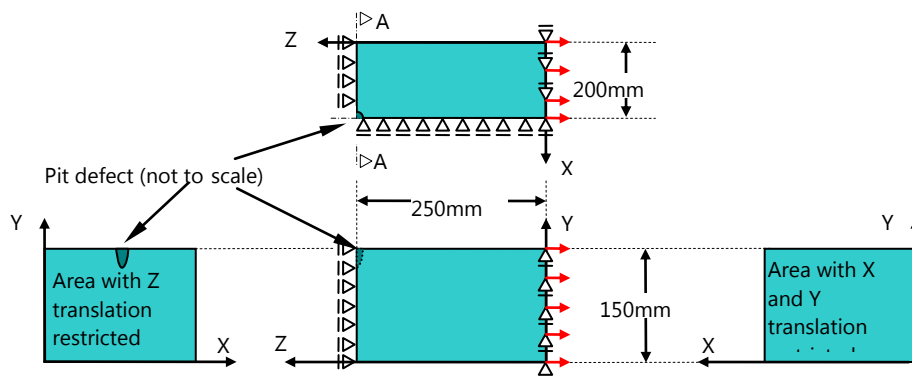


Figure 5 – ANSYS 3D model of  $\frac{1}{4}$  solid block on XYZ global coordinates.

On the pipe model depicted in Fig. 6 the longitudinal dimension is oriented along the Z direction, and the  $\frac{1}{4}$  circular ring section is placed on the XY plane. Translation restraints are applied on areas, rather than on nodes or keypoints. Area on plane XY is Z restrained. The longitudinal section on plane YZ has translation along X direction restrained. Finally, the longitudinal section on plane XZ is restrained for translation along Y direction.

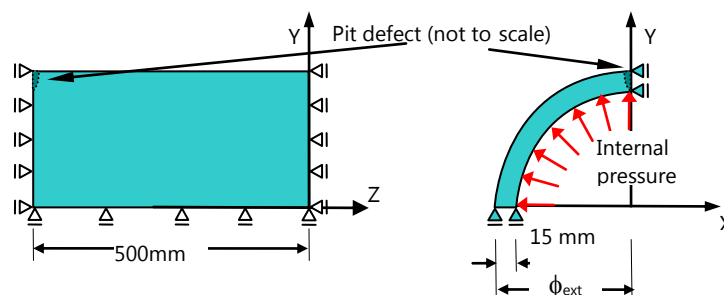


Figure 6 – 3D model of  $\frac{1}{4}$  pipe oriented along XYZ global coordinates.

Straight block analysis is done for pit diameters varying from  $50\mu\text{m}$  to 5 mm and for aspect ratio  $a/2c$  equals to 5, 4, 3, 2, 1,  $1/2$ ,  $1/3$ ,  $1/4$  e  $1/5$ , although according to Gentil (1996) a shallow defect is not considered as a pit for aspect ratios smaller than

1/2 (spherical defect). The block is loaded with tensile stresses of 10, 100, 200, 250, 300, 350, 400 and 450 MPa. Pipe analysis is done for a single pit diameter of 1 mm and for values of aspect ratio of 0.1, 0.2, 0.3, 0.4, 0.5, 1.0, 1.5, 2.0, 2.5, 3.0, 3.5 and 4.0. The quarter pipe model is loaded with internal pressures from 5 to 25 MPa.

Sometime refinement is considered to be too much trouble by beginners. It certainly increases computing time and adds complexity. However, in this particular study it is possible to demonstrate the advantages of mesh refinement when well balanced against computing effort. The region around the pit is refined in two volumes as shown in Fig. 7. The first one, closer to pit surface, is half pit diameter thick and it is composed of elements with size 1/10 of the pit diameter. The second volume is one pit diameter thick with elements approximately 1/3 of the diameter. In total a volume 1.5 radius thick has been refined. This refinement is necessary to capture not only variation on maximum stress but variation in its position. On Fig. 8 it is shown a pit with diameter of 1.5 mm and depth of 7.5 mm on a block subjected to 200 MPa of tractive tension. On the left a picture of the pit with the refined mesh. On the right the same pit with unrefined mesh. Maximum stress on refined mesh increased 8,2% over the same value of unrefined one. The position of the maximum stress, which is slightly below the mouth on the unrefined analysis, is close to the bottom when refinement is used.

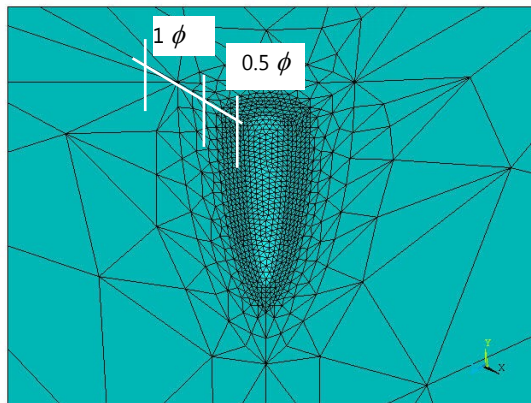


Figure 7 – Detail of refined mesh around pit in two layers.

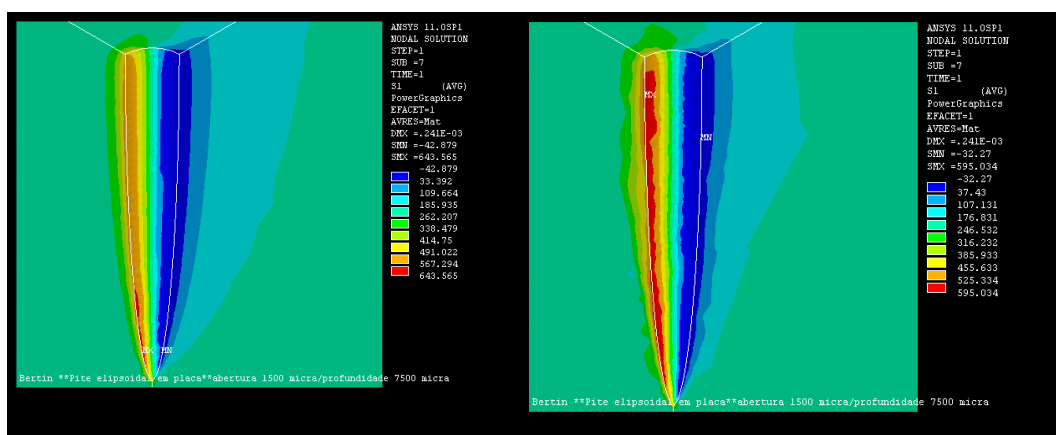


Figure 8 – Variation of maximum stress value and position due to mesh refinement. (a) refined and (b) unrefined.

## 4 RESULTS AND DISCUSSION

### 4.1 Straight Block

Results of maximum stress inside the pit for the straight block problem for applied stresses varying from 10 to 450 MPa are presented in graphic form in Fig. 9. The curves, adjusted by least square method, relate maximum stress to pit aspect ratio. Each curve represents an applied tension. The legend of the figure list all tensions used in this analysis. The logarithmic nature of the curves relates directly to the variation of the aspect ratio used, in other words, values smaller and greater than one. As expected, maximum stress increases with the increase of applied load. It is noted that close to ultimate tensile strength ( $\sigma_u = 597$  MPa) the maximum stress sometimes fluctuates, making least square adjustment less accurate. Perhaps this behavior might be accounted to the plasticity model used and the form it follows the stress – strain curve.

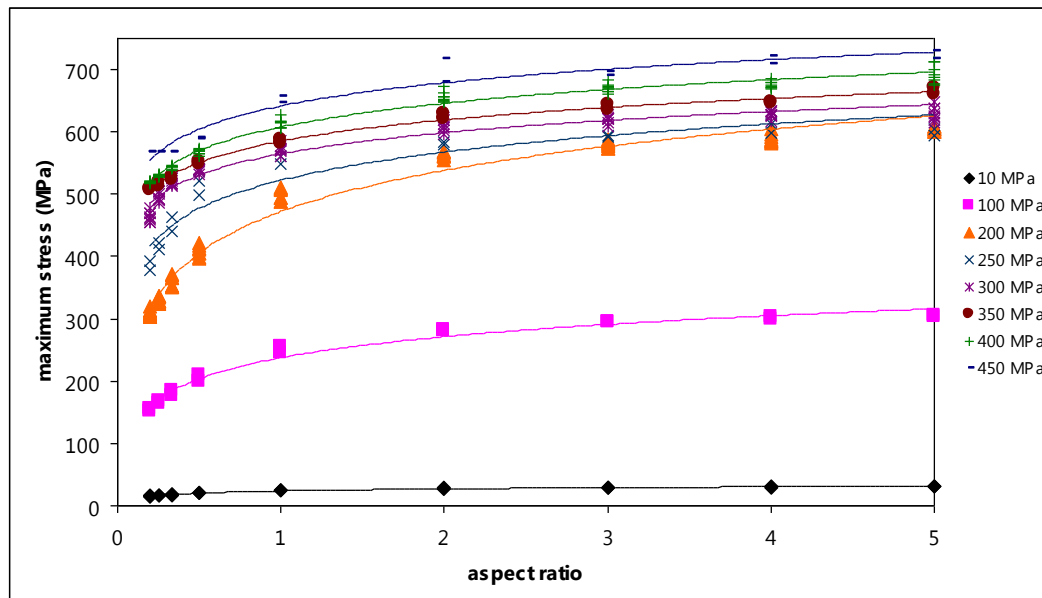


Figure 9 – Maximum stress x aspect ratio – pit on solid straight block.

The division of maximum stress data by the ultimate tensile strength leads to:

$$\frac{\sigma_{\max}}{\sigma_u} = \alpha \ln\left(\frac{a}{2c}\right) + \beta \quad (1)$$

where  $\sigma_{\max}$  is the maximum stress inside the pit;  $\sigma_u$  is the ultimate tensile strength;  $a/2c$  is the aspect ratio,  $\alpha$  is an angular parameter which controls how steep or how flat the logarithmic curve is and  $\beta$  is a linear parameter which controls the position of the 'height' of the curve so to speak. Of course angular and linear are used in analogy to the straight line function. Data of each applied tensile stress against parameters  $\alpha$  and  $\beta$  for the straight block simulations is presented in graphic form in Fig. 10.

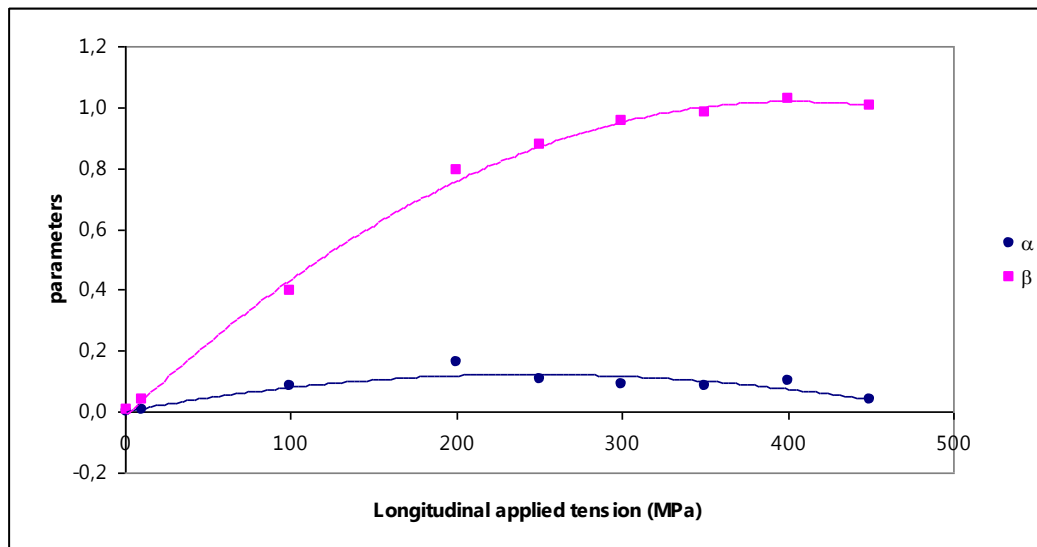


Figure 10 – Parameters  $\alpha$  and  $\beta$  for various applied longitudinal tensile stresses – plane surface

Adjustment by least square is performed leading to the following quadratic equations:

$$\begin{aligned}\alpha &= -2,017 \times 10^{-6} \sigma^2 + 9,905 \times 10^{-4} \sigma + 2,438 \times 10^{-3} \quad (R^2 = 99,8\%) \\ \beta &= -6,361 \times 10^{-6} \sigma^2 + 5,126 \times 10^{-3} \sigma - 1,268 \times 10^{-2} \quad (R^2 = 84,9\%) \end{aligned} \quad (2)$$

where  $\sigma$  is the longitudinal tensile stress applied to the block. Parentheses contain the correlation parameters.

## 4.2 Pipe

Results of maximum stress inside the pit on pipe curved surface for internal pressures from 5 to 25 MPa are presented in graphic form depicted in Fig. 11. Small bullets represent data for 300 mm diameter, medium bullets for 400 mm and large bullets depict data for 500 mm diameter pipe. Each type of bullet corresponds to an applied internal pressure. Lines just link each data point of the same kind and are not adjusted by any means unlike on the previous analysis. Two points to be noted. First the fluctuation of maximum stress values close to the ultimate tensile strength already mentioned in the block analysis. Second the increase of maximum stress inside the pit as a result of the increase of internal pressure in good relation to the analytical formulation of hoop stress:

$$\sigma_{hoop} = \frac{pd}{2t} \quad (3)$$

where  $\sigma_{hoop}$  is the hoop stress, in this case the applied stress,  $p$  is the internal pressure,  $d$  is the internal diameter of the pipe and  $t$  is the thickness of the pipe. As expected stresses inside the pit increase with the increase in pipe diameter since the applied stress is directly proportional to diameter (Eq. 3). Sometimes, as can be seen on Fig. 11, maximum stress for a bigger pipe but with smaller internal pressures

surpasses the same value for a smaller pipe with bigger pressure. Compare for instance maximum stress values of a 500mm diameter pipe subjected to 15MPa with a 300 mm one subjected to 25MPa.

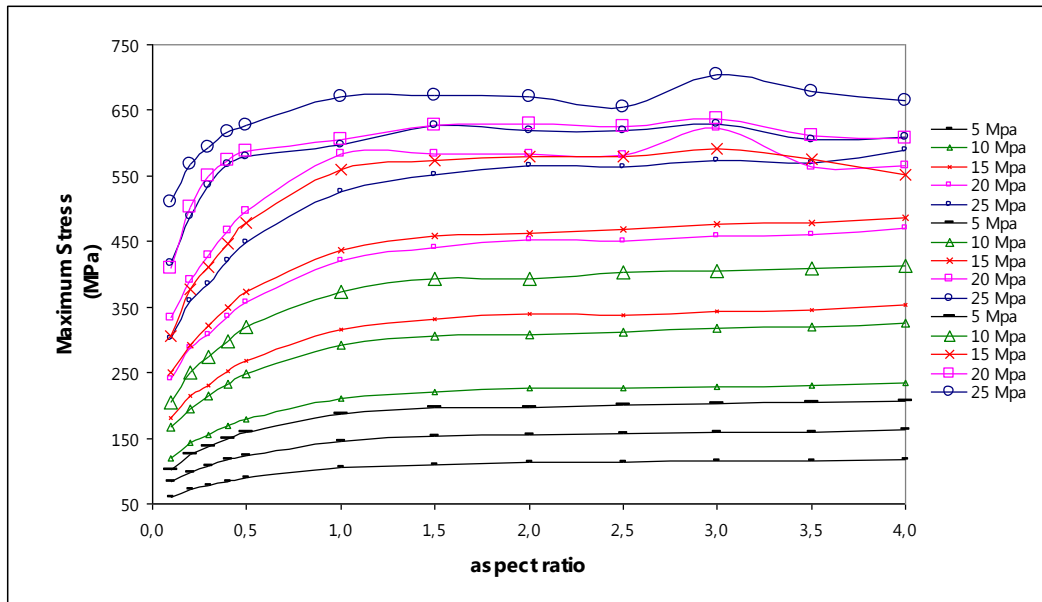


Figure 11 – Maximum stress x aspect ratio – pit on curved surface.

Similar logarithmic formulation is obtained for the pipe model analysis through a trendline analysis via least square. In this case applied hoop stress tension plotted against parameters  $\alpha$  and  $\beta$  is displayed on Fig.12. Solid lines represent the adjusted curves.

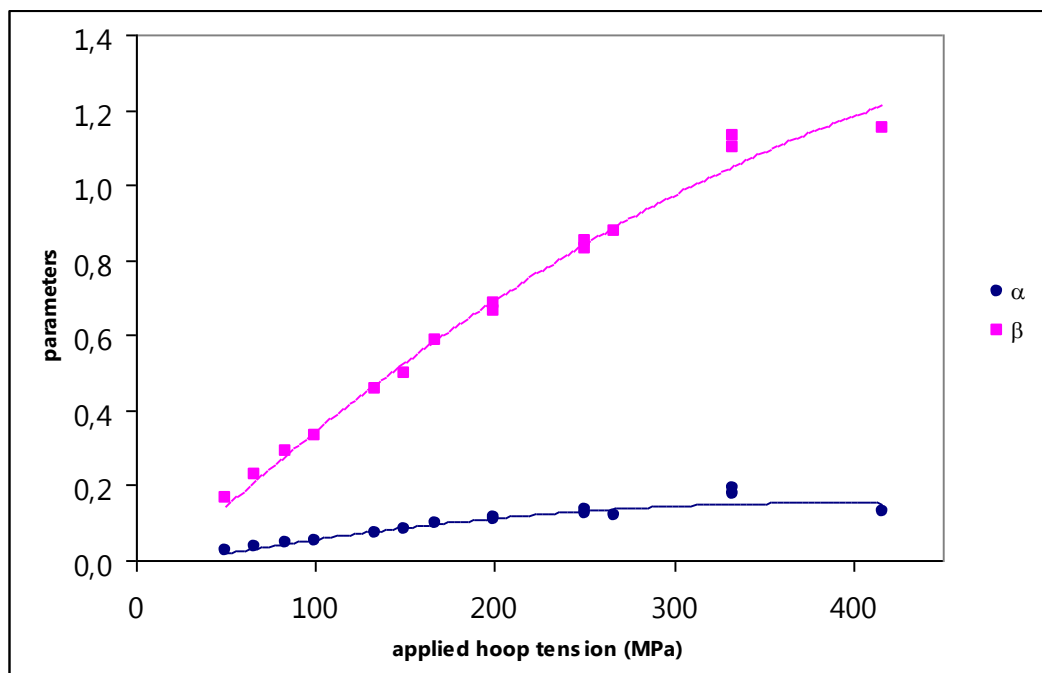


Figure 12 – Parameters  $\alpha$  and  $\beta$  for various applied hoop tensile stresses – curved surface

Adjustment by least square is performed leading to the following quadratic equations:

$$\begin{aligned}\alpha &= -3,344 \times 10^{-4} \sigma^2 + 1,604 \times 10^{-2} \sigma - 1,120 \times 10^{-2} \quad (R^2 = 90,5\%) \\ \beta &= -5,068 \times 10^{-5} \sigma^2 + 7,559 \times 10^{-2} \sigma - 2,232 \times 10^{-2} \quad (R^2 = 98,8\%)\end{aligned}\quad (4)$$

where  $\sigma$  is the hoop stress resulting from internal pressure (Eq. 3).

Placing all data of  $\alpha$  and  $\beta$  pertaining to both analyses on the same graphic (see Fig. 13) allows the following equations:

$$\begin{aligned}\alpha &= -4,070 \times 10^{-6} \sigma^2 + 4,529 \times 10^{-3} \sigma - 3,848 \times 10^{-2} \quad (R^2 = 98,1\%) \\ \beta &= -1,368 \times 10^{-6} \sigma^2 + 8,723 \times 10^{-4} \sigma - 7,588 \times 10^{-3} \quad (R^2 = 75,5\%)\end{aligned}\quad (3)$$

where  $\sigma$  is the applied stress.

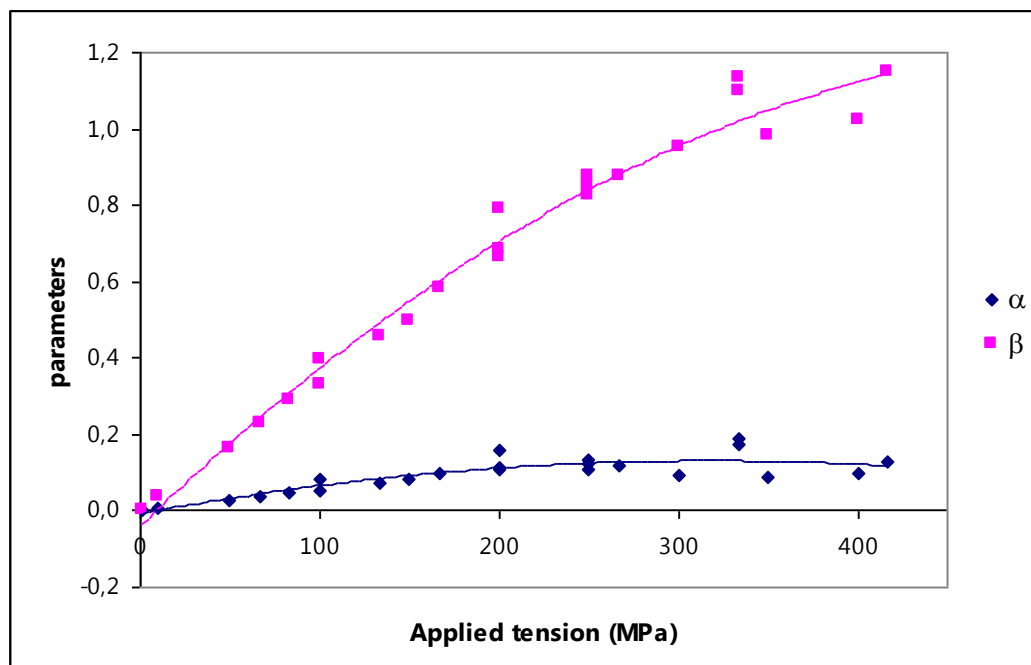


Figure 13 – Parameters  $\alpha$  and  $\beta$  for applied tension – flat and curved surface

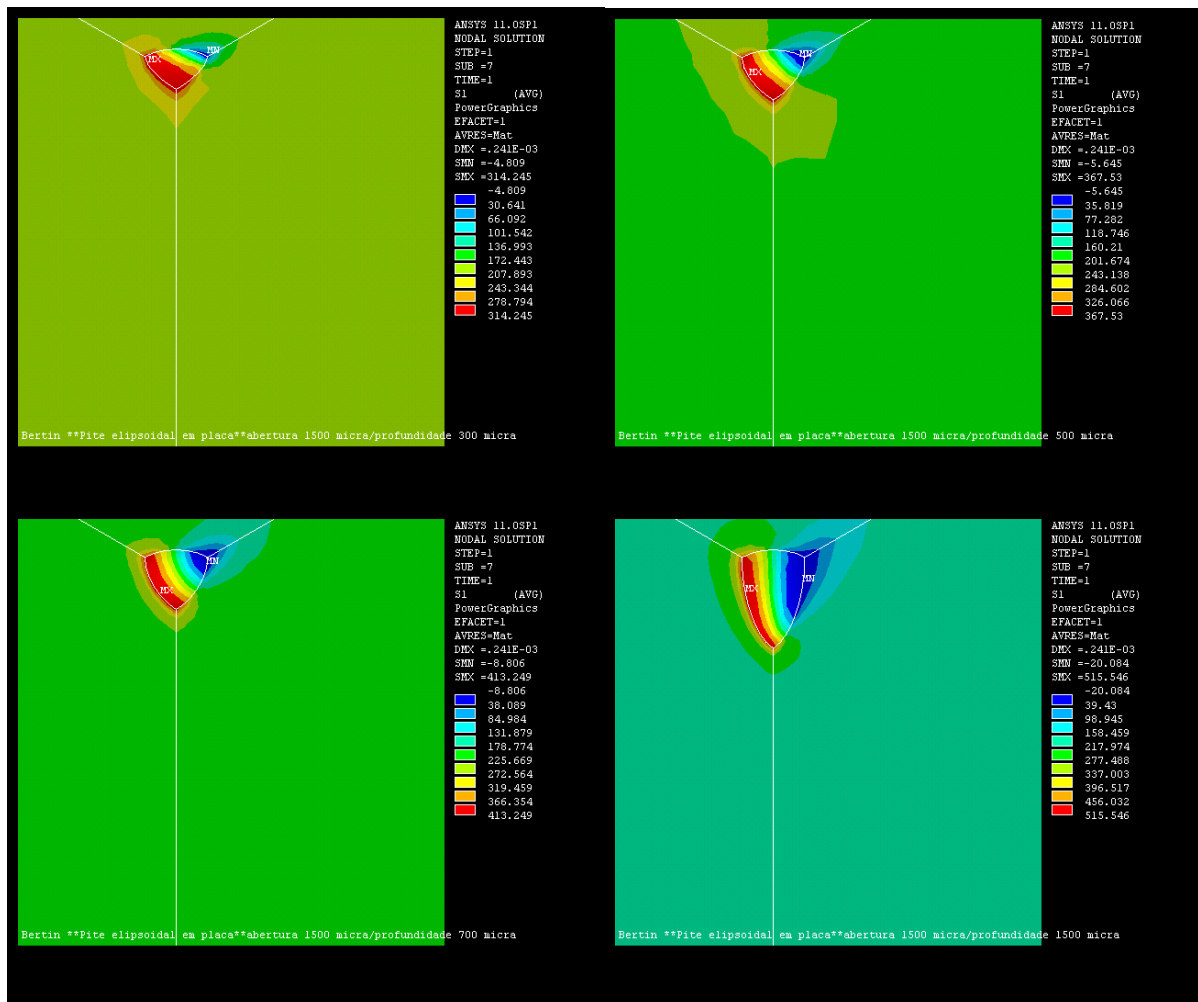
### 4.3 Distribution of stress inside the pit

Distributions of stress inside a corrosion pit 1.5 mm diameter on a straight block subjected to longitudinal tension of 200 MPa, with aspect ratios of 0.2, 0.33, 0.47, 1.0, 2.1, 3.0, 4.1 and 5.0 are shown on Figs. 14 and 15. For values of stress below yield point, in other words, before plastification, maximum stress occurs as a uniform (red) band. However as maximum stress surpasses yield stress, as pit depth increases to 1.5 mm (aspect ratio = 1.0) and greater values, that band narrows considerably as plastification occurs and finally rupture if that option was allowed by the software.

Turnbull, Horner, and Connolly (2009) did 3-D X-ray tomographic images of pits on a “turbine disc steel exposed to a simulated condensate environment” and concluded

that "the crack initiates near the mouth of the pit". Therefore also of some importance is the position of maximum stress inside the corrosion pit. For shallow pits ( $a/2c < 1$ ) and even for a pit with  $a/2c = 1$  maximum stress locates close to the pit mouth, but as depth increases its position moves closer to the bottom of the pit.

Distributions of stress inside a corrosion pit 1.0 mm diameter on a curved pipe like surface 300 mm of diameter, subjected to internal pressure of 25 MPa, with aspect ratios of 0.2, 0.3, 0.4, 0.5, 1.0, 2.0, 3.0 and 4.0 are shown on Figs. 16 and 17. Similar to the straight block simulation, or values of stress bellow yield point, maximum stress occurs as a (red) band larger at the bottom and narrower at the mouth of the pit. However as maximum stress surpasses yield stress, as pit depth increases to 1.0 mm (aspect ratio =1.0) and greater, that band narrows considerably as effect of plastification.



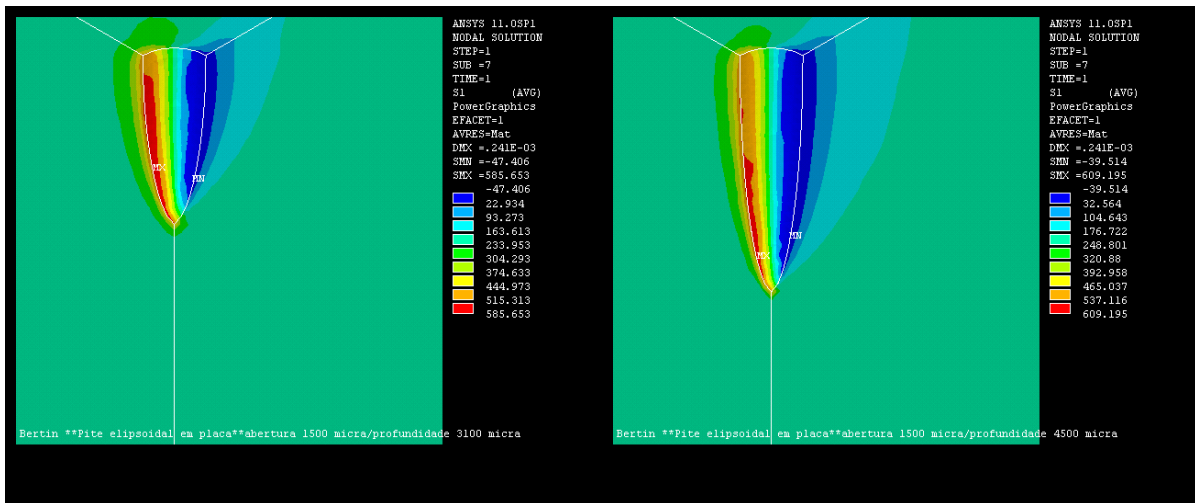


Figure 14 – Distribution of stress inside a corrosion pit on a straight block subjected to longitudinal tension of 200 MPa, with aspect ratios 0.2, 0.33, 0.47, 1.0, 2.1 and 3.0

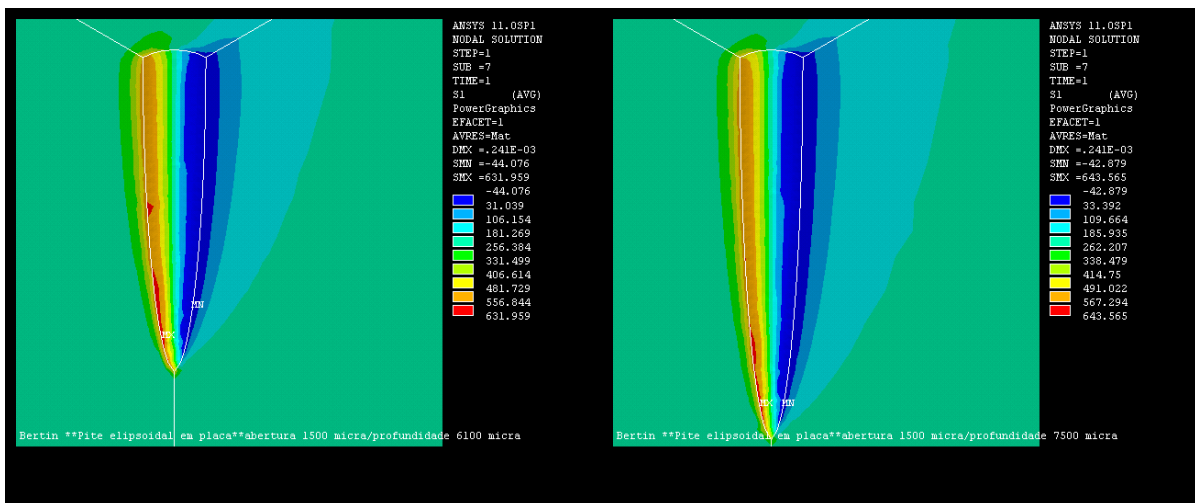


Figure 15 – Distribution of stress inside a corrosion pit on a straight block subjected to longitudinal tension of 200 MPa, with aspect ratios 4.1 and 5.0

On curved surfaces the stress intensification effect is increased greatly. In this case even for a low aspect ratio of 0.3 maximum stress locates at the bottom of the pit where it stays up to aspect ratios of 2.0. Although for aspect ratio of 3.0 and 4.0 maximum stress is positioned a little bit above the bottom this might be regarded as a failure of the plasticity model to follow the stress – strain curve, as mentioned before. In fact, for the internal pressure simulated, 25 MPa, ultimate strength value of 597 MPa is reached at aspect ratio of 2.0, therefore a greater value should be expected at aspect ratio of 3.0. However for the last maximum stress obtained is only 590 MPa. The same occurs with diameters of 400 and 500 mm, except that yield and rupture points occurs at smaller aspect ratios.

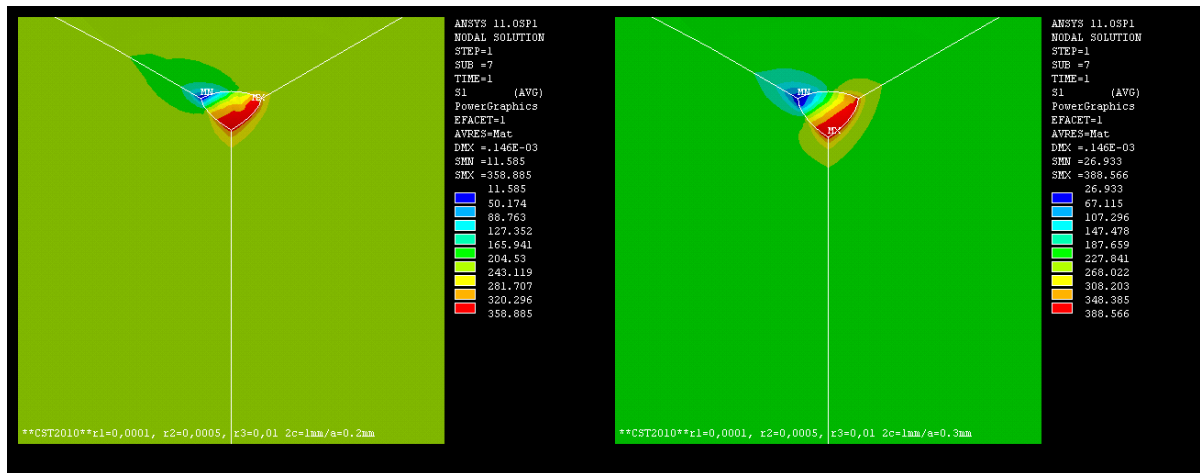
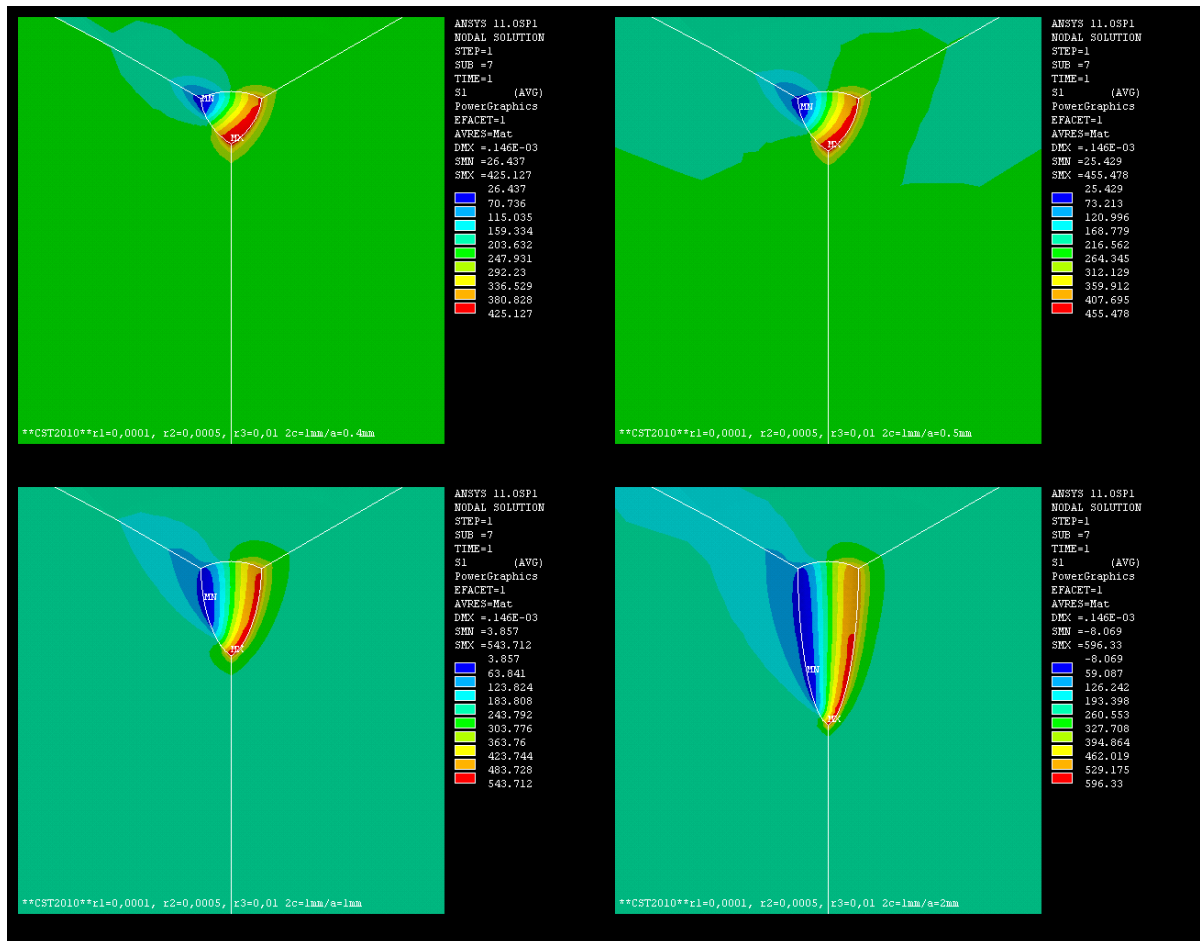


Figure 16 – Distribution of stress inside a corrosion pit on a curved surface 300 mm diameter subjected to internal pressure of 25 MPa, with aspect ratios 0.2 and , 0.3



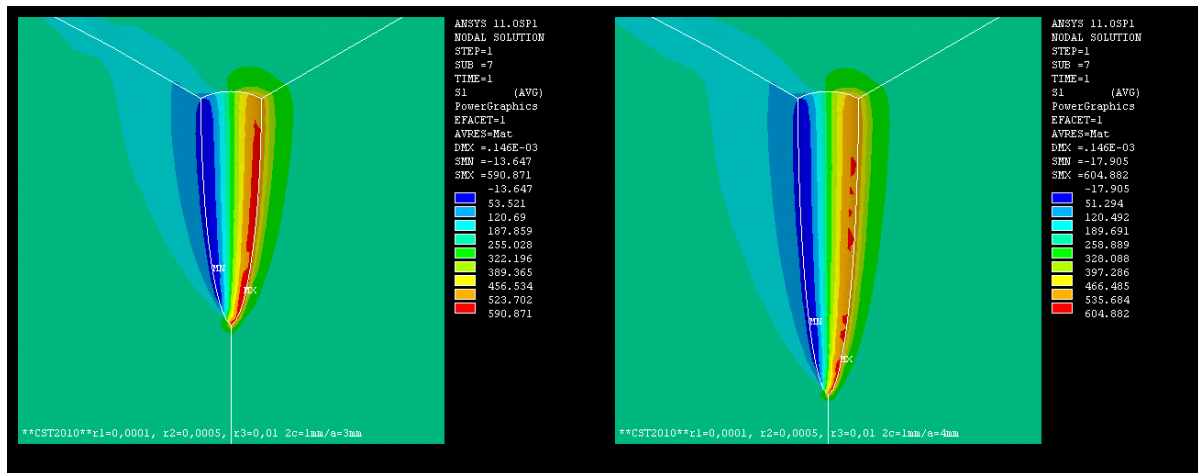


Figure 17 – Distribution of stress inside a corrosion pit on a curved surface 300 mm diameter subjected to internal pressure of 25 MPa, with aspect ratios 0.4, 0.5, 1.0, 2.0, 3.0 and 4.0

## 5 CONCLUSION

This work had the objective of comparing maximum stress inside corrosion pits on both plane and curved surfaces subjected to tensile stress considering plasticity of the material. Analysis were carried out using the finite element program ANSYS®. It was possible to obtain a logarithmic expression involving maximum stress, ultimate tensile strength, applied stress and pit aspect ratio with good correlation. Stress distribution inside the corrosion pit are also shown. Further research might be done to integrate Young's modulus and Poisson's ration in the formulation.

## REFERENCES

- Bertin, R.J., Abdalla Filho, J.E. and Machado, R.D., *Stress analysis of corrosion pits present on pipeline surfaces*. XXX CILAMCE, 2009
- Callister, W. D., *Fundamentos da ciência e engenharia de materiais: uma abordagem integrada* (2ª ed.). (S. M. SOARES, Trans.) Rio de Janeiro: LTC - Livros Técnicos e Científicos Editora S.A., p. 503, 2006.
- Cerit, M., Genel, K. and Eksi, S., Numerical investigation on stress concentration of corrosion pit. *Engineering Failure Analysis*, 16: 2467–2472, 2009.
- Gentil, Vicente, *Corrosão*. Rio de Janeiro: Livros Técnicos e Científicos Editora S.A., p. 39,1996.
- Pao, P.S., Gill, S.J. and Feng, C.R., On fatigue crack initiation from corrosion pits in 7075-t7351 aluminum alloy. *Scripta Materialia*, 43: 391-396, 2000.
- Turnbull, A., McCartney, L.N. and Zhou, S., Modeling of the evolution of stress corrosion cracks from corrosion pits. *Scripta Materialia*, 54: 575-578, 2008.
- Turnbull, A., Horner, D.A. and Connolly, B.J., Challenges in modelling the evolution of stress corrosion cracks from pits. *Engineering Fracture Mechanics*, 76: 633-640, 2009.